

Observation of $B \rightarrow \phi K$ and $B \rightarrow \phi K^*$

R. A. Briere,¹ G. P. Chen,¹ T. Ferguson,¹ H. Vogel,¹ A. Gritsan,² J. P. Alexander,³ R. Baker,³ C. Bebek,³ B. E. Berger,³ K. Berkelman,³ F. Blanc,³ V. Boisvert,³ D. G. Cassel,³ P. S. Drell,³ J. E. Duboscq,³ K. M. Ecklund,³ R. Ehrlich,³ P. Gaidarev,³ L. Gibbons,³ B. Gittelman,³ S. W. Gray,³ D. L. Hartill,³ B. K. Heltsley,³ P. I. Hopman,³ L. Hsu,³ C. D. Jones,³ J. Kandaswamy,³ D. L. Kreinick,³ M. Lohner,³ A. Magerkurth,³ T. O. Meyer,³ N. B. Mistry,³ E. Nordberg,³ M. Palmer,³ J. R. Patterson,³ D. Peterson,³ D. Riley,³ A. Romano,³ J. G. Thayer,³ D. Urner,³ B. Valant-Spaight,³ G. Viehhauser,³ A. Warburton,³ P. Avery,⁴ C. Prescott,⁴ A. I. Rubiera,⁴ H. Stoeck,⁴ J. Yelton,⁴ G. Brandenburg,⁵ A. Ershov,⁵ D. Y.-J. Kim,⁵ R. Wilson,⁵ T. Bergfeld,⁶ B. I. Eisenstein,⁶ J. Ernst,⁶ G. E. Gladding,⁶ G. D. Gollin,⁶ R. M. Hans,⁶ E. Johnson,⁶ I. Karliner,⁶ M. A. Marsh,⁶ C. Plager,⁶ C. Sedlack,⁶ M. Selen,⁶ J. J. Thaler,⁶ J. Williams,⁶ K. W. Edwards,⁷ R. Janicek,⁸ P. M. Patel,⁸ A. J. Sadoff,⁹ R. Ammar,¹⁰ A. Bean,¹⁰ D. Besson,¹⁰ X. Zhao,¹⁰ S. Anderson,¹¹ V. V. Frolov,¹¹ Y. Kubota,¹¹ S. J. Lee,¹¹ J. J. O'Neill,¹¹ R. Poling,¹¹ T. Riehle,¹¹ A. Smith,¹¹ C. J. Stepaniak,¹¹ J. Urheim,¹¹ S. Ahmed,¹² M. S. Alam,¹² S. B. Athar,¹² L. Jian,¹² L. Ling,¹² M. Saleem,¹² S. Timm,¹² F. Wappler,¹² A. Anastassov,¹³ E. Eckhart,¹³ K. K. Gan,¹³ C. Gwon,¹³ T. Hart,¹³ K. Honscheid,¹³ D. Hufnagel,¹³ H. Kagan,¹³ R. Kass,¹³ T. K. Pedlar,¹³ H. Schwarthoff,¹³ J. B. Thayer,¹³ E. von Toerne,¹³ M. M. Zoeller,¹³ S. J. Richichi,¹⁴ H. Severini,¹⁴ P. Skubic,¹⁴ A. Undrus,¹⁴ V. Savinov,¹⁵ S. Chen,¹⁶ J. Fast,¹⁶ J. W. Hinson,¹⁶ J. Lee,¹⁶ D. H. Miller,¹⁶ E. I. Shibata,¹⁶ I. P. J. Shipsey,¹⁶ V. Pavlunin,¹⁶ D. Cronin-Hennessy,¹⁷ A. L. Lyon,¹⁷ E. H. Thorndike,¹⁷ T. E. Coan,¹⁸ V. Fadeyev,¹⁸ Y. S. Gao,¹⁸ Y. Maravin,¹⁸ I. Narsky,¹⁸ R. Stroynowski,¹⁸ J. Ye,¹⁸ T. Wlodek,¹⁸ M. Artuso,¹⁹ C. Boulahouache,¹⁹ K. Bukin,¹⁹ E. Dambasuren,¹⁹ G. Majumder,¹⁹ R. Mountain,¹⁹ S. Schuh,¹⁹ T. Skwarnicki,¹⁹ S. Stone,¹⁹ J. C. Wang,¹⁹ A. Wolf,¹⁹ J. Wu,¹⁹ S. Kopp,²⁰ M. Kostin,²⁰ A. H. Mahmood,²¹ S. E. Csorna,²² I. Danko,²² K. W. McLean,²² Z. Xu,²² R. Godang,²³ G. Bonvicini,²⁴ D. Cinabro,²⁴ M. Dubrovin,²⁴ S. McGee,²⁴ G. J. Zhou,²⁴ A. Bornheim,²⁵ E. Lipeles,²⁵ S. P. Pappas,²⁵ M. Schmidler,²⁵ A. Shapiro,²⁵ W. M. Sun,²⁵ A. J. Weinstein,²⁵ D. E. Jaffe,²⁶ R. Mahapatra,²⁶ G. Masek,²⁶ H. P. Paar,²⁶ D. M. Asner,²⁷ A. Eppich,²⁷ T. S. Hill,²⁷ and R. J. Morrison²⁷

(CLEO Collaboration)

¹*Carnegie Mellon University, Pittsburgh, Pennsylvania 15213*

²*University of Colorado, Boulder, Colorado 80309-0390*

³*Cornell University, Ithaca, New York 14853*

⁴*University of Florida, Gainesville, Florida 32611*

⁵*Harvard University, Cambridge, Massachusetts 02138*

⁶*University of Illinois, Urbana-Champaign, Illinois 61801*

⁷*Carleton University, Ottawa, Ontario, Canada K1S 5B6
and the Institute of Particle Physics, Canada*

⁸*McGill University, Montréal, Québec, Canada H3A 2T8
and the Institute of Particle Physics, Canada*

⁹*Ithaca College, Ithaca, New York 14850*

¹⁰*University of Kansas, Lawrence, Kansas 66045*

¹¹*University of Minnesota, Minneapolis, Minnesota 55455*

¹²*State University of New York at Albany, Albany, New York 12222*

¹³*The Ohio State University, Columbus, Ohio 43210*

¹⁴*University of Oklahoma, Norman, Oklahoma 73019*

¹⁵*University of Pittsburgh, Pittsburgh, Pennsylvania 15260*

¹⁶*Purdue University, West Lafayette, Indiana 47907*

¹⁷*University of Rochester, Rochester, New York 14627*

¹⁸*Southern Methodist University, Dallas, Texas 75275*

¹⁹*Syracuse University, Syracuse, New York 13244*

²⁰*University of Texas, Austin, Texas 78712*

²¹*University of Texas-Pan American, Edinburg, Texas 78539*

²²*Vanderbilt University, Nashville, Tennessee 37235*

²³*Virginia Polytechnic Institute and State University, Blacksburg, Virginia 24061*

²⁴*Wayne State University, Detroit, Michigan 48202*

²⁵*California Institute of Technology, Pasadena, California 91125*

²⁶*University of California, San Diego, La Jolla, California 92093*

²⁷*University of California, Santa Barbara, California 93106*

(Received 18 January 2001)

We have studied two-body charmless hadronic decays of B mesons into the final states ϕK and ϕK^* . Using 9.7 million $B\bar{B}$ pairs collected with the CLEO II detector, we observe the decays $B^- \rightarrow \phi K^-$ and $B^0 \rightarrow \phi K^{*0}$ with the following branching fractions: $\mathcal{B}(B^- \rightarrow \phi K^-) = (5.5_{-1.8}^{+2.1} \pm 0.6) \times 10^{-6}$ and $\mathcal{B}(B^0 \rightarrow \phi K^{*0}) = (11.5_{-3.7}^{+4.5+1.8}) \times 10^{-6}$. We also see evidence for the decays $B^0 \rightarrow \phi K^0$ and $B^- \rightarrow \phi K^{*-}$. However, since the statistical significance is not overwhelming for these modes, we determine upper limits of $<12.3 \times 10^{-6}$ and $<22.5 \times 10^{-6}$ (90% confidence level), respectively.

DOI: 10.1103/PhysRevLett.86.3718

PACS numbers: 13.25.Hw

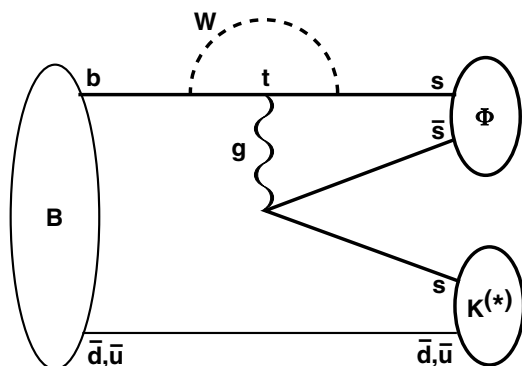
The phenomenon of CP violation can be accommodated in the standard model (SM) by a complex phase in the Cabibbo-Kobayashi-Maskawa (CKM) quark-mixing matrix [1]. Whether this phase is the only source of CP violation in nature remains an open experimental question. Studies of charmless B meson decays will certainly play an important role in constraining the CKM matrix and testing the SM picture of CP violation.

Flavor changing neutral currents (FCNC) are forbidden to first order in the SM. Second order loop diagrams, known as penguin and box diagrams, can generate effective FCNC which lead to $b \rightarrow s$ transitions. These processes are of considerable interest because they are sensitive to V_{ts} , the CKM matrix element which will be very difficult to measure in direct decays of the top quark. They are also sensitive to nonstandard model physics [2], since charged Higgs bosons, new gauge bosons, or supersymmetric particles can contribute via additional loop diagrams.

Among final states produced by the gluonic penguin, $b \rightarrow sg$, decay modes in which a gluon splits into two strange quarks, $g \rightarrow s\bar{s}$, play a special role since they cannot be produced by any other b decay with comparable rate, thus providing an unambiguous signature for the gluonic penguin. As illustrated in Fig. 1, a particularly clean final state is produced when the kaon includes the spectator quark and no pions are emitted.

In this Letter we present the first significant measurements of exclusive charmless hadronic decays $B \rightarrow \phi K$ and $B \rightarrow \phi K^*$. Measurements of other charmless hadronic decay modes by CLEO are discussed elsewhere [3].

The data set used in this analysis was collected with the CLEO detector at the Cornell Electron Storage Ring (CESR). It consists of 9.13 fb^{-1} taken at the $\Upsilon(4S)$

FIG. 1. Penguin diagram describing $B \rightarrow \phi K^{(*)}$ decays.

(on-resonance), corresponding to $9.66M B\bar{B}$ pairs, and 4.35 fb^{-1} taken below $B\bar{B}$ threshold, used for continuum background studies.

CLEO II is a general purpose solenoidal magnet detector [4]. Cylindrical drift chambers in a 1.5 T solenoidal magnetic field measure momentum and specific ionization (dE/dx) of charged particles. Photons are detected using a 7800-crystal CsI(Tl) electromagnetic calorimeter. In the CLEO II.V detector configuration, the innermost chamber was replaced by a three-layer, double-sided silicon vertex detector, and the gas in the main drift chamber was changed from an argon-ethane to a helium-propane mixture. As a result of these modifications, the CLEO II.V portion of the data (2/3 of the total) has improved particle identification and momentum resolution.

In the analysis presented here we search for B meson decays by selecting ϕ and K (K^*) decay candidates using specific criteria. Track quality requirements are imposed on charged tracks, and pions and kaons are identified by dE/dx . Electrons are rejected based on dE/dx and the ratio of the track momentum to the associated shower energy in the CsI calorimeter; muons are rejected based on their penetration depth in the instrumented steel flux return. The K_S^0 candidates are selected from $\pi^+\pi^-$ pairs forming well-measured secondary vertices with invariant mass within 3 standard deviations (σ) of the nominal K_S^0 mass and a decay path significance of at least 3σ . The neutral pion candidates are formed from pairs of isolated photonlike energy clusters in the CsI calorimeter with invariant mass within -3.5 and $+3.0$ standard deviations of the π^0 mass. The ϕ meson candidates have K^+K^- mass within $\pm 20 \text{ MeV}/c^2$ ($\pm 4.5\Gamma$, $\Gamma =$ natural width) of the known ϕ mass, and the specific ionization of the tracks is consistent with the K^+K^- hypothesis. The K^* candidates are reconstructed in four modes: $K^{*0} \rightarrow K^-\pi^+$, $K^{*0} \rightarrow K^0\pi^0$, $K^{*-} \rightarrow K^-\pi^0$, and $K^{*-} \rightarrow K^0\pi^-$, and their masses lie within $\pm 75 \text{ MeV}/c^2$ ($\pm 1.5\Gamma$) of the respective known masses. Charmless two-body B decays produce the fastest secondary particles among all B decays. Therefore, to reduce combinatoric backgrounds only the fastest ϕ and the fastest K (K^*) are used in those events with multiple combinations.

The B decay candidate is identified via its invariant mass and its total energy. We calculate a beam-constrained B mass $M_B = \sqrt{E_{\text{beam}}^2 - p_B^2}$, where p_B is the B candidate momentum and E_{beam} is the beam energy. The resolution in M_B is dominated by the beam energy spread. We define $\Delta E = E_1 + E_2 - E_{\text{beam}}$, where E_1 and E_2 are the

energies of the daughters of the B meson candidate. We accept events with M_B above $5.2 \text{ GeV}/c^2$ and $|\Delta E| < 200 \text{ MeV}$.

We have studied backgrounds from $b \rightarrow c$ decays and other $b \rightarrow u$ and $b \rightarrow s$ decays and find that all are negligible for the analyses presented here. The main background arises from $e^+e^- \rightarrow q\bar{q}$ (where $q = u, d, s, c$). Such events typically exhibit a two-jet structure and can produce high momentum back-to-back tracks in the fiducial region, while $B\bar{B}$ events tend to have more spherical structure, since the B mesons are produced nearly at rest. To reduce contamination from these background events, we require the event to have $H_2/H_0 < 0.6$, where H_i are Fox-Wolfram moments [5].

We extract the signal yields from unbinned, extended maximum-likelihood fits of the preselected on-resonance data separately for each topology (ϕK^- , ϕK^0 , $\phi K_{\rightarrow K^-\pi^+}^{*0}$, $\phi K_{\rightarrow K^0\pi^0}^{*0}$, $\phi K_{\rightarrow K^-\pi^0}^{*-}$, $\phi K_{\rightarrow K^0\pi^-}^{*-}$). For all modes, we distinguish signal from background using M_B , ΔE , $|\cos\theta_{II}|$ (the angle between the thrust axes of the B candidate and that of the rest of the event), $|\cos\theta_B|$ (the angle between the B candidate momentum and beam axis), and m_ϕ (the mass of the ϕ candidate). In addition, we include $|\cos\theta_h|$ (the ϕ helicity angle, defined as the kaon direction in the ϕ rest frame) for ϕK^- and ϕK^0 modes, m_{K^*} (the mass of the K^* candidate) for ϕK^* modes, and S_K (the number of standard deviations from the predicted dE/dx value) of K^- when applicable.

In each of these fits, the likelihood of the event is the sum of probabilities for the signal and background hypotheses, with relative weights determined by maximizing the likelihood function \mathcal{L} . The probability of a particular hypothesis is calculated as a product of the probability density functions (PDFs) for each of the input variables. The signal PDFs are represented by a double Gaussian for M_B and ΔE , by a Breit-Wigner function on top of a linear polynomial for m_ϕ and m_{K^*} , by $1 - |\cos\theta_B|^2$ for $|\cos\theta_B|$, by a third order polynomial for $|\cos\theta_{II}|$, and by $\cos^2\theta_h$ for $|\cos\theta_h|$. The background distributions for the intermediate resonance masses are parametrized by the sum of a Breit-Wigner and a low-order polynomial. For M_B , we use an empirical shape ($f(M_B) \propto M_B \sqrt{1 - x^2} \exp[-\gamma(1 - x^2)]$; $x = M_B/E_{\text{beam}}$) [6]. The background ΔE and $|\cos\theta_B|$ PDFs are both linear functions, and $|\cos\theta_{II}|$ is parametrized by the sum of two terms $|\cos\theta_{II}|^\alpha$ with different exponents. The signal and background dependences of S_K are bifurcated Gaussian functions.

The parameters for the PDFs are determined from off-resonance data (background) and from high-statistics Monte Carlo (MC) samples (signal). In the signal MC data, we model $B \rightarrow \phi K^{(*)}$ as a two-body decay, where for ϕK^* we assume equal amplitudes for longitudinal and transverse polarizations. Dependence on the unknown decay polarization is included in the systematic uncertainty. We use a Geant [7] based simulation to model the detector response in detail. Further

details about the likelihood fit method can be found in Ref. [8].

To illustrate the fits, we show in Fig. 2 M_B and ΔE projections for the modes with significant signals.

Events entering these plots must satisfy a requirement on the signal-to-background likelihood ratios $R \equiv \log(P_{si}/P_{bi})$, where P_{si} (P_{bi}) are signal (background) likelihoods for each event i , computed without M_B and ΔE , respectively. This additional cut accepts about 2/3 of the preselected signal events in the MC sample.

We summarize the results for all B decay modes, corresponding submodes, and the combined modes in Table I, where we assume equal branching fractions for charged and neutral B meson decays [9].

We combine the samples from multiple secondary decay channels by adding the $-2 \log \mathcal{L}$ functions of the branching fraction. The statistical significance of a given signal yield is determined from the change in $-2 \log \mathcal{L}$ when refit with the signal yield fixed to zero. The largest contributions to the systematic uncertainties come, with about equal weight, from uncertainties in the parametrization of the PDFs, decay polarization dependence, and possible background from other B decays. [The $B \rightarrow \phi K^*$ decay may be longitudinally or transversely polarized. Assuming 100% transverse polarization we obtain $\mathcal{B}(B \rightarrow \phi K^*) = (13.6^{+5.3}_{-4.4}) \times 10^{-6}$ (statistical errors only) and $\mathcal{B}(B^- \rightarrow \phi K^{*-}) = (12.8^{+7.6}_{-5.9}) \times 10^{-6}$. Assuming 100%

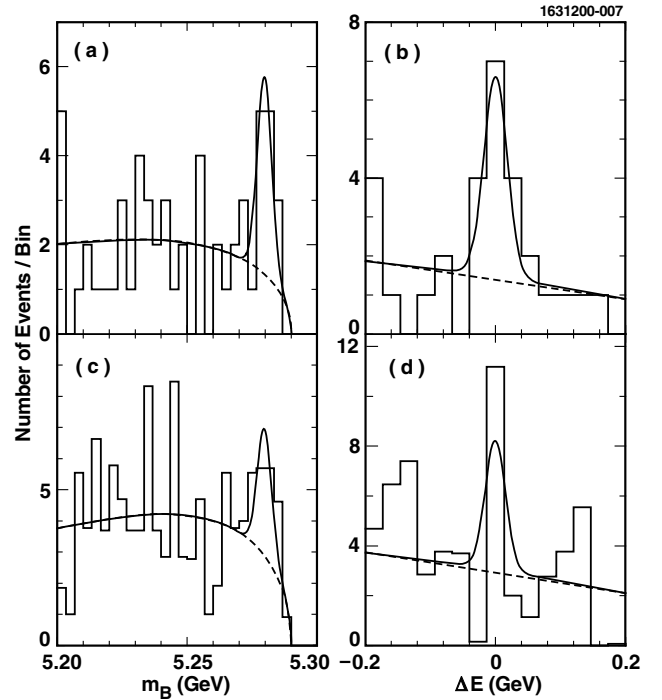


FIG. 2. M and ΔE plots for (a),(b) $B^- \rightarrow \phi K^-$, and (c),(d) $B^0 \rightarrow \phi K^*$ after the requirement on R as described in the text. The projection of the total likelihood fit (solid curve) and the continuum background component (dashed curve) are overlaid. For $B^0 \rightarrow \phi K^{*0}$, the two decay modes of K^{*0} were weighted according to the statistical errors of the fits.

TABLE I. Intermediate fitted branching fractions (\mathcal{B}_{fit}), final branching fraction results (\mathcal{B}), and theoretical estimates [10] are given in units of 10^{-6} . When the result is not statistically significant, the final result is quoted as a 90% confidence level (C.L.) upper limit. The errors on branching fractions are statistical and systematic, respectively. Reconstruction efficiency ϵ does not include branching fractions, and it is quoted for modes with K^0 assuming $K^0 \rightarrow K_S^0 \rightarrow \pi^+ \pi^-$ decay.

Mode	Yield	ϵ (%)	\mathcal{B}_{fit}	Stat. signif.	\mathcal{B}	Theory \mathcal{B}
ϕK^-	$14.2_{-4.5}^{+5.5}$	54	$5.5_{-1.8}^{+2.1} \pm 0.6$	5.4σ	See \mathcal{B}_{fit}	0.7–16
ϕK^0	$4.2_{-2.1}^{+2.9}$	48	$5.4_{-2.7}^{+3.7} \pm 0.7$	2.9σ	<12.3	0.7–13
ϕK comb.	6.1σ	$5.5_{-1.5}^{+1.8} \pm 0.7$	
$\phi K^{*0} (K^- \pi^+)$	$12.1_{-4.3}^{+5.3}$	38	$9.9_{-3.5-1.6}^{+4.3+1.6}$	4.5σ	...	
$\phi K^{*0} (K^0 \pi^0)$	$5.1_{-2.8}^{+3.9}$	20	$46.3_{-26.0-6.6}^{+35.7+5.9}$	2.7σ	...	
ϕK^{*0}	$11.5_{-3.7-1.7}^{+4.5+1.8}$	5.1σ	See \mathcal{B}_{fit}	0.2–31
$\phi K^{*-} (K^- \pi^0)$	$3.8_{-2.8}^{+4.1}$	25	$9.3_{-7.0-1.5}^{+10.1+1.7}$	1.5σ	...	
$\phi K^{*-} (K^0 \pi^-)$	$4.0_{-2.2}^{+3.1}$	32	$11.4_{-6.3-1.8}^{+9.0+1.8}$	2.7σ	...	
ϕK^{*-}	$10.6_{-4.9-1.6}^{+6.4+1.8}$	3.1σ	<22.5	0.2–31
ϕK^* comb.	5.9σ	$11.2_{-3.1-1.7}^{+3.6+1.8}$	

longitudinal polarization we measure $\mathcal{B}(B \rightarrow \phi K^*) = (9.9_{-3.4}^{+4.2}) \times 10^{-6}$ and $\mathcal{B}(B^- \rightarrow \phi K^{*-}) = (9.9_{-4.6}^{+6.0}) \times 10^{-6}$. To estimate the uncertainty due to the unknown polarization we assumed that any value between 100% longitudinal and 100% transverse polarization is equally likely.]

We observe a significant signal (above 5σ) for the decays $B^- \rightarrow \phi K^-$ and $B^0 \rightarrow \phi K^{*0}$. Since the statistical significances for the $B^0 \rightarrow \phi K^0$ and $B^- \rightarrow \phi K^{*-}$ modes are not large (2.9σ and 3.1σ , respectively), we calculate 90% C.L. upper limits by integrating the likelihood curve to 90% of its total area and increasing it by one unit of the systematic error.

In summary, we have measured $\mathcal{B}(B^- \rightarrow \phi K^-) = (5.5_{-1.8}^{+2.1} \pm 0.6) \times 10^{-6}$ and $\mathcal{B}(B^0 \rightarrow \phi K^{*0}) = (11.5_{-3.7-1.7}^{+4.5+1.8}) \times 10^{-6}$ each with statistical significance above 5σ . The statistical significance of the $B^0 \rightarrow \phi K^0$ and $B^- \rightarrow \phi K^{*-}$ signals are 2.9σ and 3.1σ , respectively. The measured rates are $\mathcal{B}(B^0 \rightarrow \phi K^0) = (5.4_{-2.7}^{+3.7} \pm 0.7) \times 10^{-6}$ and $\mathcal{B}(B^- \rightarrow \phi K^{*-}) = (10.6_{-4.9-1.6}^{+6.4+1.8}) \times 10^{-6}$. Since the statistical significance in these modes is limited we set upper limits of $<12.3 \times 10^{-6}$ and $<22.5 \times 10^{-6}$ (at 90% C.L.), respectively. Averaging over B^0 and B^- we obtain $\mathcal{B}(B \rightarrow \phi K) = (5.5_{-1.5}^{+1.8} \pm 0.7) \times 10^{-6}$ (6.1σ) and $\mathcal{B}(B \rightarrow \phi K^*) = (11.2_{-3.1-1.7}^{+3.6+1.8}) \times 10^{-6}$ (5.9σ). The measured branching fractions lie in the range of theoretical predictions (see Table I). Since there is a considerable spread in theoretical predictions among various calculations, our results will help constrain model parameters.

We gratefully acknowledge the effort of the CESR staff in providing us with excellent luminosity and running conditions. This work was supported by the National Science Foundation, the U.S. Department of Energy, the Research Corporation, the Natural Sciences and Engineering Research Council of Canada, the Swiss National Science Foundation, the Texas Advanced

Research Program, and the Alexander von Humboldt Stiftung.

- [1] M. Kobayashi and K. Maskawa, Prog. Theor. Phys. **49**, 652 (1973).
- [2] See, for example, J.L. Hewett and J.D. Wells, Phys. Rev. D **55**, 5549 (1997); G. Burdman, Phys. Rev. D **52**, 6400 (1995); N.G. Deshpande, K. Panose, and J. Trampetić, Phys. Lett. B **308**, 322 (1993); W.S. Hou, R.S. Willey, and A. Soni, Phys. Rev. Lett. **58**, 1608 (1987).
- [3] CLEO Collaboration, R. Godang *et al.*, Phys. Rev. Lett. **80**, 3456 (1998); CLEO Collaboration, B.H. Behrens *et al.*, Phys. Rev. Lett. **80**, 3710 (1998); CLEO Collaboration, T. Bergfeld *et al.*, Phys. Rev. Lett. **81**, 272 (1998); CLEO Collaboration, D. Cronin-Hennessy *et al.*, Phys. Rev. Lett. **85**, 515 (2000); CLEO Collaboration, S.J. Richichi *et al.*, Phys. Rev. Lett. **85**, 520 (2000); CLEO Collaboration, C.P. Jessop *et al.*, Phys. Rev. Lett. **85**, 2881 (2000).
- [4] CLEO Collaboration, Y. Kubota *et al.*, Nucl. Instrum. Methods Phys. Res., Sect. A **320**, 66 (1992); T.S. Hill, Nucl. Instrum. Methods Phys. Res., Sect. A **418**, 32 (1998).
- [5] G. Fox and S. Wolfram, Phys. Rev. Lett. **41**, 1581 (1978).
- [6] ARGUS Collaboration, H. Albrecht *et al.*, Phys. Lett. B **241**, 278 (1990); ARGUS Collaboration, H. Albrecht *et al.*, Phys. Lett. B **254**, 288 (1991).
- [7] R. Brun *et al.*, CERN DD/EE/84-1.
- [8] CLEO Collaboration, D.M. Asner *et al.*, Phys. Rev. D **53**, 1039 (1996).
- [9] CLEO Collaboration, J.P. Alexander *et al.*, Phys. Rev. Lett. (to be published), Report No. CLNS 00/1670, CLEO 00-7.
- [10] N.G. Deshpande and J. Trampetić, Phys. Rev. D **41**, 895 (1990); L.-L. Chau *et al.*, Phys. Rev. D **43**, 2176 (1991); A. Deandrea *et al.*, Phys. Lett. B **318**, 549 (1993); A. Deandrea *et al.*, Phys. Lett. B **320**, 170 (1994); A.J. Davies, T. Hayashi, M. Matsuda, and M. Tanimoto, Phys. Rev. D **49**, 5882 (1994); G. Kramer, W.F. Palmer, and H. Simma, Nucl. Phys. **B428**, 77 (1994); G. Kramer, W.F. Palmer, and H. Simma, Z. Phys. C **66**, 429 (1995); D. Du and L. Guo, Z. Phys. C **75**, 9 (1997).